

## Facile Fabrication of Pt-Cu Nanoclusters-Decorated Porous Poly(5-cyanoindole) with High Electrocatalytic Activity

Fengxing Jiang<sup>1,2</sup>, Rong Zhou<sup>1,3</sup>, Zhangquan Yao<sup>1,3</sup>, Yukou Du<sup>1,\*</sup>, Jingkun Xu<sup>2,\*</sup>, Ping Yang<sup>1</sup>, Chuanyi Wang<sup>3,\*</sup>

<sup>1</sup> College of Chemistry, Chemical Engineering and Materials Science, Soochow University, Suzhou 215123, PR China.

<sup>2</sup> Jiangxi Key Laboratory of Organic Chemistry, Jiangxi Science and Technology Normal University, Nanchang 330013, PR China.

<sup>3</sup> Xinjiang Technical Institute of Physics & Chemistry, Chinese Academy of Sciences, Urumqi 830011, PR China.

\*E-mail: [duyk@suda.edu.cn](mailto:duyk@suda.edu.cn) (Y. Du), [xujingkun@tsinghua.org.cn](mailto:xujingkun@tsinghua.org.cn) (J. Xu), [cywang@ms.xjb.ac.cn](mailto:cywang@ms.xjb.ac.cn) (C. Wang).

Received: 1 July 2011 / Accepted: 12 August 2011 / Published: 1 September 2011

---

Poly(5-cyanoindole) (P5CN), an excellent electron and proton conducting polymer, was incorporated with highly dispersed and small sized Pt-Cu nanoclusters on a glassy carbon (GC) electrode by electrochemical co-electrodeposition. The Pt-Cu nanoclusters-decorated P5CN (Pt-Cu/P5CN/GC) shows remarkable electrocatalytic activity toward methanol and formic acid oxidation in acid medium. The morphological characterizations by the scanning electron microscopy (SEM) and transmission electron microscopy (TEM) demonstrate the porous structure of P5CN and good dispersion of Pt-Cu nanoclusters with small diameter. The energy dispersive X-ray spectroscopy (EDX) and X-ray photoelectron spectrometer (XPS) also confirm the components of Pt-Cu/P5CN composites and their electronic structures. The cyclic voltammetric and chronoamperometric methods were used to investigate the catalytic activity and stability of as-prepared catalysts. The experimental results indicate that the P5CN as support and Cu introduced into Pt enhance the catalytic activity.

---

**Keywords:** Poly(5-cyanoindole), Co-electrodeposition, Nanocluster, Electrocatalytic activity, Acid medium.

### 1. INTRODUCTION

Currently, direct methanol fuel cells (DMFC) and direct formic acid fuel cells (DFAFC) have received much attention around this world because of the sustainable energy and environmental

concern. Platinum as an electrocatalyst is one of the most common precious metals with extraordinary catalytic activity in the application of fuel cells. A large number of researches have been focused on the Pt-based (Pt-M, M=Ni, Mn, Co and Cu *et al.*) catalysts in order to reduce the expensive Pt cost and improve the catalytic activity of Pt-M nanoparticles (NPs) [1-6]. Up to now, the superior electrocatalytic activity of Pt-M NPs catalyst has been demonstrated compared to pure Pt NPs for methanol and formic acid electrooxidation [2, 5, 7]. The enhanced catalytic activity can be attributed to the electronic and structural effects by the addition of certain metal in Pt NPs [3, 7]. Among these Pt-M NPs catalysts, Pt-Cu NPs showed unique catalytic activity for methanol and formic acid oxidation [1-3].

As is also known, the electrocatalytic activity depends on not only the structure of atoms on the surface of Pt-M NPs, but also the ratio of surface area to volume and the dispersion of catalysts [8, 9]. In other words, the small-sized and well-dispersed catalysts with the same overall volume can show the large electrochemical surface area, which is favorable for the catalytic activity. Generally, the well-dispersed Pt or Pt-M NPs need the aid of a conductive support as electrocatalysts [9-11]. Therefore, many alternative conductive materials have been studied as the support of catalyst to achieve a high catalytic activity, such as carbon blacks, carbon nanotubes and conducting polymers (CPs). Page *et al.* [12] studied the Pt-Cu/C catalysts with a low onset potential for methanol oxidation compared to Pt/C, Pt-Co/C and Pt-Ni/C. Yen and co-workers reported that the Pt-Cu NPs on multiwalled carbon nanotubes (MWCNTs) have a low onset potential, whereas the lower peak current for methanol oxidation than the pure Pt/MWCNTs [4]. However, little research has been conducted in the CPs-supported Pt-Cu NPs catalysts for methanol and formic acid oxidation.

CPs incorporated with noble metals as electrocatalysts have been widely investigated in fuel cells in recent years, which is due to their porous structures, high surface areas and access to many catalytic sites [13-19]. More importantly, some CPs such as polyaniline (PANi), polypyrrole (PPy) and polyindole (PIn), are excellent electron and proton conducting materials. The feature probably makes CPs to provide enhanced performance for the catalyst in fuel cell electrode [11]. Patra and Munichandraiah pointed out that CPs as support can not only efficiently disperse Pt NPs, but also improve the interfacial properties between the electrode and the electrolyte and allow a facile flow of electronic charges during the process of electrochemical oxidation on Pt NPs [14]. Poly(5-cyanoindole) (P5CN) is one of the excellent CPs with the good electron and proton conducting properties, it shows good stability in air and optical properties [19-21]. Moreover, the presence of cyano group in the P5CN can enhance the dispersion of metallic NPs and the preferentially sufficient deposition site [22, 23]. Zhou and co-workers have also demonstrated the Pt/P5CN composite has a high efficient electrocatalytic oxidation for formic acid [13, 24]. In previous works, many of Pt/CPs composites showed the enhanced electrocatalytic activity for the methanol and formic acid oxidation [24-27]. However, the Pt NPs obtained by electrochemical method in the CPs matrixes showed the large size in diameter (*ca.* 20~100 nm) with the small ratio of surface area to volume. Therefore, it is desirable to well disperse and reduce the size of Pt NPs in CPs matrixes.

In the present work, we employed P5CN as a matrix to disperse Pt-Cu nanoclusters for methanol and formic acid electrooxidation by a facile co-electrodeposition. The preparation of metallic nanoclusters in CPs matrixes have been accepted for the development of electrocatalytic materials [28,

29]. Moreover, co-electrodeposition has been demonstrated to be an available method for the formation of metallic nanoclusters by using Cu sacrificial adlayers as a template [29, 30]. Here, our particular interest is mainly focused on the improvement of dispersed Pt-Cu nanoclusters and the increase of electrochemical surface area of Pt-Cu nanoclusters. To achieve well-dispersed Pt-Cu nanoclusters on the surface of P5CN, the co-electrodeposition were carried out in the 1.0 mM  $\text{H}_2\text{PtCl}_6$  + 1.0 mM  $\text{CuSO}_4$  + 0.5 M  $\text{H}_2\text{SO}_4$  by cyclic voltammetry. The catalytic activity of as-prepared catalyst was detected by cyclic voltammetric and chronoamperometric methods.

## 2. EXPERIMENTAL

### 2.1. Materials

All the chemical reagents used in this study were analytical grade. 5-cyanoindole (5CN) and tetrabutylammonium tetrafluoroborate ( $\text{Bu}_4\text{NBF}_4$ ) were purchased from Acros. Hexachloroplatinic acid hexahydrate ( $\text{H}_2\text{PtCl}_6 \cdot 6\text{H}_2\text{O}$ ), copper sulphate pentahydrate ( $\text{CuSO}_4 \cdot 5\text{H}_2\text{O}$ ), boron trifluoride diethyl ether (BFEE), diethyl ether (EE), sulfuric acid ( $\text{H}_2\text{SO}_4$ ), methanol ( $\text{CH}_3\text{OH}$ ) and formic acid ( $\text{HCOOH}$ ) were used in our study from Sinopharm Chemical Reagent Co. Ltd. The BFEE and EE were distilled before use. All aqueous solutions were prepared with double distilled water.

### 2.2. Fabrication of catalysts

In terms of fabricating catalysts, we adopted a two-step synthetical method with use of CHI 660B electrochemical working station (CH Instrument, Inc.). A glassy carbon electrode (GC, 3 mm diameter) and Pt wire were used as the working electrode and counter electrode, respectively. Before the experiments, the GC was polished down to  $0.03 \mu\text{m}$ , and then rinsed thoroughly with doubly distilled water in an ultrasonic bath. Initially, poly(5-cyanoindole)-modified glassy carbon electrode (P5CN/GC) was prepared by using 5CN as a chemical precursor. In short, P5CN was synthesized by cyclic voltammetry from 0.1 V to 1.4 V vs. SCE (saturated calomel electrode) at  $50 \text{ mV s}^{-1}$  in a typical electrolytic solution of 50% BFEE and 50% EE containing  $0.05 \text{ mol L}^{-1} \text{ Bu}_4\text{NBF}_4$  and  $0.05 \text{ mol L}^{-1} \text{ 5CN}$ . The as-prepared P5CN/GC electrode was rinsed by EE and washed repeatedly with water for next experiments.

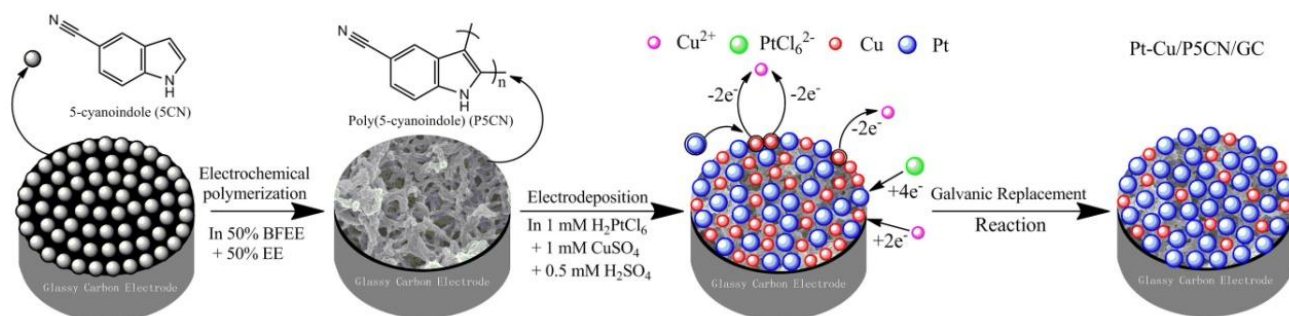


**Figure 1.** Scheme for the synthesis of Pt-Cu/P5CN/GC.

The Pt and Pt-Cu nanoclusters were obtained by using cyclic voltammetry between -0.25 V and 0.5 V *vs.* SCE at 50 mV s<sup>-1</sup> in 1.0 mM H<sub>2</sub>PtCl<sub>6</sub> and 0.5 M H<sub>2</sub>SO<sub>4</sub> solution with and without 1.0 mM CuSO<sub>4</sub>, respectively. In order to obtain a better stable Pt-Cu nanocluster-decorated P5CN/GC (Pt-Cu/P5CN/GC), the as-prepared Pt-Cu/P5CN/GC was kept into the electrolytic solution for 30 min after the deposition of Pt-Cu so that the Cu atoms on the surface of Pt-Cu were completely replaced by Pt. Simultaneously, to better understand the effect of P5CN in the process of electrocatalytic oxidation, Pt/GC, Pt-Cu/GC and Pt/P5CN/GC were prepared as comparison. The detailed process is depicted in Fig. 1.

### 2.3. Characterization

The morphology and microstructure of the as-prepared P5CN and Pt-Cu/P5CN/GC were investigated by scanning electron microscopy (SEM), energy dispersive X-ray spectroscopy (EDX) and transmission electron microscopy (TEM). The surface structures of as-prepared catalysts were analyzed with a KRATOS X-ray photoelectron spectrometer (XPS).

### 2.4. Electrochemical measurements

All electrochemical measurements were performed on a CHI 660B potentiostat with a standard three-electrode configuration. The Pt or Pt-Cu with and without P5CN-modified GC electrodes prepared above was used as the working electrode. All potentials in present study were given *vs.* SCE reference electrode. Prior to the measurements, the solutions were deoxygenated by bubbling with high-purity N<sub>2</sub> for 30 min. Cyclic voltammetry (CV) was carried out in the solution of 0.5 mol L<sup>-1</sup> H<sub>2</sub>SO<sub>4</sub>, 0.5 mol L<sup>-1</sup> H<sub>2</sub>SO<sub>4</sub> + 0.5 mol L<sup>-1</sup> CH<sub>3</sub>OH, 0.5 mol L<sup>-1</sup> H<sub>2</sub>SO<sub>4</sub> + 0.5 mol L<sup>-1</sup> HCOOH, respectively.

## 3. RESULTS AND DISCUSSION

### 3.1. Preparation, morphology and structure characterization

The morphologies and microstructures of as-prepared Pt-Cu/P5CN/GC catalysts were investigated by SEM and TEM. Fig. 2 (A and B) shows a representative SEM micrograph for the P5CN (A) and Pt-Cu/P5CN (B) on GC electrode. The P5CN obtained by CVs exhibited 3D porous nanostructure, and provided a high specific surface area for electrochemical reactions, which may be a good candidate as the support material. In the present study, Pt-Cu particles were nucleated and distributed in the P5CN matrix in nanoscale dimensions. The porous nanostructure of P5CN was decorated with a thickness of Pt-Cu particles. The Pt-Cu nanoclusters were prepared by co-electrodeposition in the 1.0 mM H<sub>2</sub>PtCl<sub>6</sub> + 1.0 mM CuSO<sub>4</sub> + 0.5 M H<sub>2</sub>SO<sub>4</sub>. The EDX analysis showed that the Pt-Cu/P5CN was composed of Pt and Cu elements in an atomic ratio close to 4:1 in Fig. 2C. Xu *et al.* [3] indicated that the Pt<sub>80</sub>Cu<sub>20</sub> nanocubes had the best electrocatalytic activity compared to

other Pt:Cu ratio. Simultaneously, TEM images (Fig. 2D and E) revealed that the Pt-Cu particles exhibited nanocluster morphologies and had a narrow size distribution on the surface of P5CN. Interestingly, the Pt-Cu nanoclusters were well-dispersed on the surface of P5CN and had no aggregation into large particles.

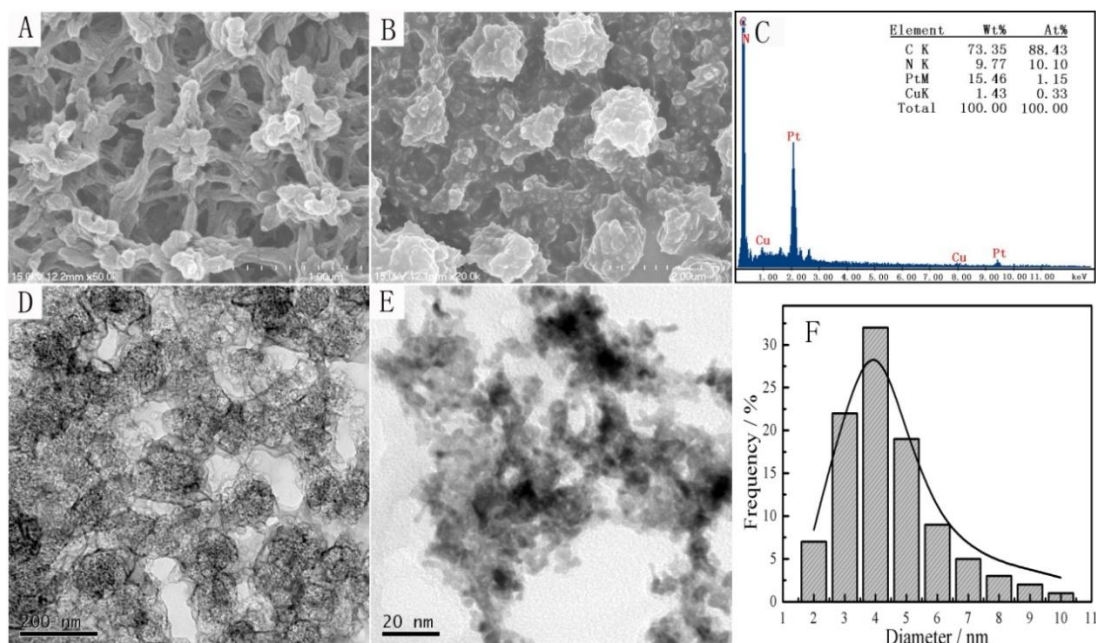


**Figure 2.** Representative SEM micrographs of P5CN (A), Pt-Cu/P5CN (B) and the EDX analysis (C) of Pt-Cu/P5CN/GC obtained from B. TEM images (D and E) of Pt-Cu/P5CN and the diameter size distribution (F) obtained from E.

The formation of Pt-Cu nanoclusters is directly related to the presence of  $\text{Cu}^{2+}$  ions during the process of co-electrodeposition. The Cu atom on the surface of P5CN plays a crucial role, and thoroughly replaced by Pt atoms based on the galvanic replacement reaction:



The overall co-electrodeposition of Pt-Cu nanoclusters is also similar to copper underpotential deposition, and the Cu was sacrificed as a reversibly deposited mediator [30-32]. Sieradzki *et al.* [33] pointed out that the deposition and stripping of a mediator metal by appropriate cycling of the electrochemical potential can create new nuclei on the surface and add to the existing clusters on the surface. Huang *et al.* [34] prepared Pt-Cu NPs on the MWCNTs/Au by potentiostatic method at -0.2 V and then at 0.6 V for Cu electrochemical stripping with a large size of Pt-Cu NPs (*ca.* 100 nm).

For the well-dispersed Pt-Cu nanoclusters, the formed porous P5CN played an important role and made the Pt-Cu nanoclusters to effectively avoid possible agglomeration [14, 35]. Fig. 2F shows the diameter size distribution histogram of nanoclusters depicted in Fig. 2E. A normal distribution fit to the histogram yielded a mean particle size of 4.5 nm, which is particularly desirable to

electrocatalytic activity. Additionally, methanol and formic acid oxidation strongly depend on the particle size of Pt NPs. Park *et al.* [36] reported methanol and formic acid electrooxidation exhibited similar activity with Pt nanoparticles larger than 4 nm which avoided the size effect that methanol electrooxidation show decreased activity with a smaller size than 4 nm.

XPS spectrum (Fig. 3) was further conducted to investigate the atomic composition and the oxidation states of the atom in Pt-Cu/P5CN/GC. As shown in Fig. 3A, the curve fitting of the  $C_{1s}$  XPS spectrum consists of three peaks at 284.44, 284.98 and 286.15 eV, which can be attributed to the C-C, C=C, C-H, and C-N,  $C\equiv N$ , and the oxidized carbon species such as C-O bond, respectively [15, 37]. Fig. 3B presents the deconvolution of  $N_{1s}$  core level spectrum with two main binding energy peak at 399.8 and 401.58 eV. It is suggested that the binding energy peak centred at 399.8 eV may be assigned to the benzenoid structure of P5CN, while the high intensity peak at 401.58 eV is probably due to the nitrogen cationic radical ( $N^+$ ) according to literatures [37, 38]. This result indicated the P5CN has a typical electronic structure. The characteristic peak of  $Pt_{4f}$  at 71.1 eV revealed the presence of metallic Pt in Fig. 3C. Additionally, the binding energy peak at 74.8 eV may be corresponding to PtO and PtO<sub>2</sub> [39]. However, No significant amounts Cu can be detected on the surface of Pt-Cu nanoclusters in Fig. 3D, which indicates that the existent Cu atoms in Pt-Cu/P5CN/GC are embedded into the Pt-Cu nanoclusters.

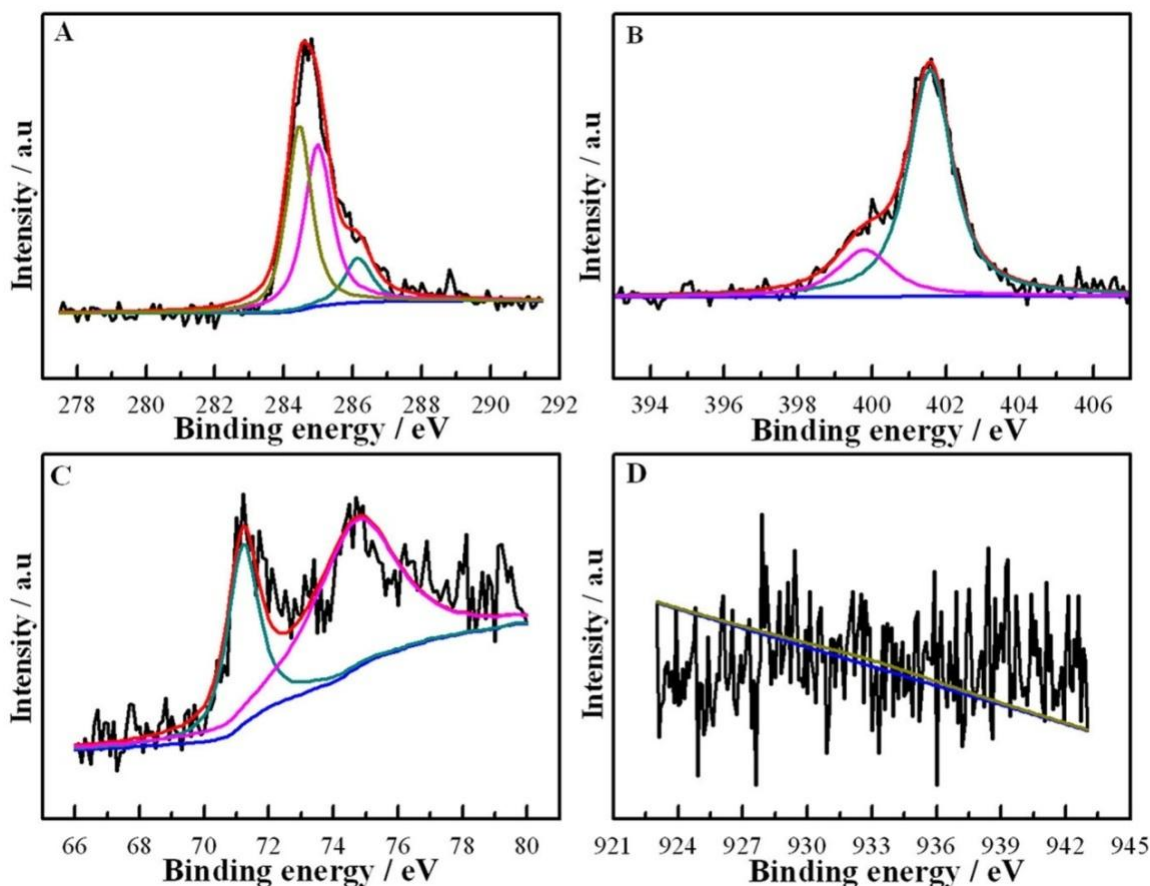


**Figure 3.** XPS spectrum of Pt-Cu/P5CN showing the characteristic binding energy peak for  $C_{1s}$  (A),  $N_{1s}$  (B),  $Pt_{4f}$  (C) and  $Cu_{2p}$  (D), respectively.

## 3.2. Electrochemical behaviour characterization

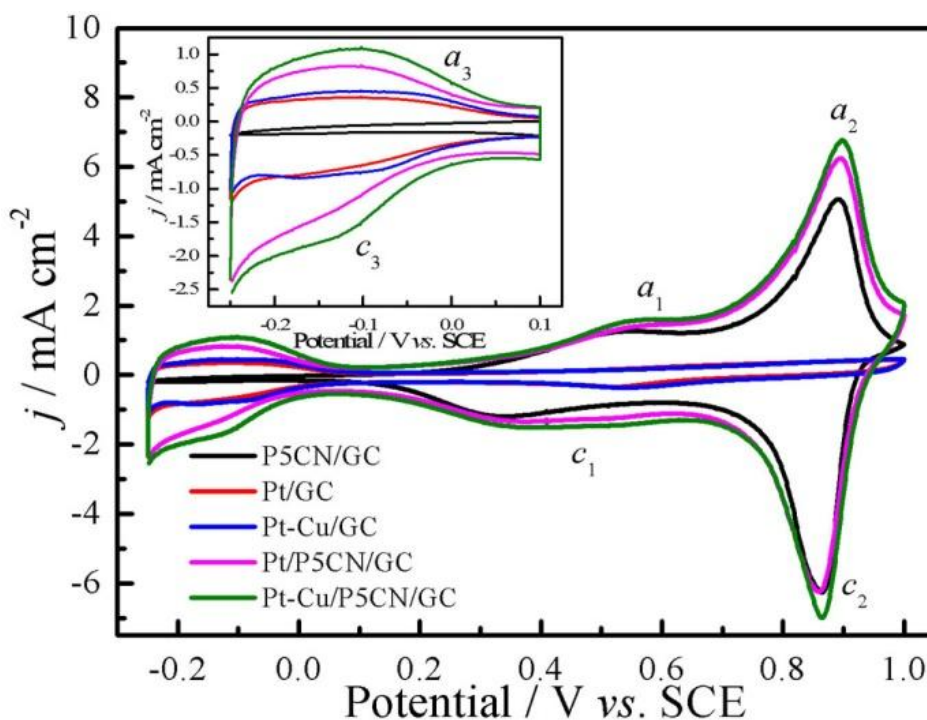


**Figure 4.** CVs of P5CN/GC, Pt/GC, Pt-Cu/GC, Pt/P5CN/GC and Pt-Cu/P5CN/GC in 0.5 mol L<sup>-1</sup> H<sub>2</sub>SO<sub>4</sub> at the scan rate of 50 mV s<sup>-1</sup>. Inset: the amplifying images between -0.25 and 0.1 V.

It is well known that the electrocatalytic performance of as-prepared catalysts can be explored for the by evaluating their potential in anode catalysts technology [40]. Fig. 4 shows the CVs of different catalysts in 0.5 mol L<sup>-1</sup> H<sub>2</sub>SO<sub>4</sub> solution. The CVs profiles are characterized by a typical hydrogen region, electrochemical double-layer, metal particles and polymer redox behaviours. It can be seen that at the P5CN/GC, the voltammogram displays two pair of distinctive electrochemical redox peaks (*a*<sub>1</sub>, *c*<sub>1</sub>) and (*a*<sub>2</sub>, *c*<sub>2</sub>).

The similar electrochemical feature of P5CN has been observed in HCl and HClO<sub>4</sub> solution by Talbi and co-workers [20]. The first peak (*a*<sub>1</sub>, *c*<sub>1</sub>) between 0.15 and 0.65 V presents the electron exchange of P5CN during the first redox process in Fig. 5, while the second peak (*a*<sub>2</sub>, *c*<sub>2</sub>) is mainly attributed to the proton exchange related to the redox transformation between 0.65 and 1.0 V in Fig. 5, whereas no obvious peak current can be observed between -0.25 and 0.05 V.

The intense peaks indicate that the P5CN is an excellent electron and proton conducting materials. Additionally, at Pt-Cu/P5CN/GC, the voltammetric peaks at both (*a*<sub>1</sub>, *c*<sub>1</sub>) and (*a*<sub>2</sub>, *c*<sub>2</sub>) are relatively higher than these at P5CN/GC, which suggests that the electron transfer kinetics are markedly enhanced by the incorporation of Pt or Pt-Cu nanoclusters on the P5CN surface layer. Additionally, there is no Cu dissolution to be detected from the CVs of Pt-Cu/GC and Pt-Cu/P5CN/GC, which is in agreement with the result of XPS and indicates the Pt-Cu nanoclusters have Pt-rich shell on their surfaces.

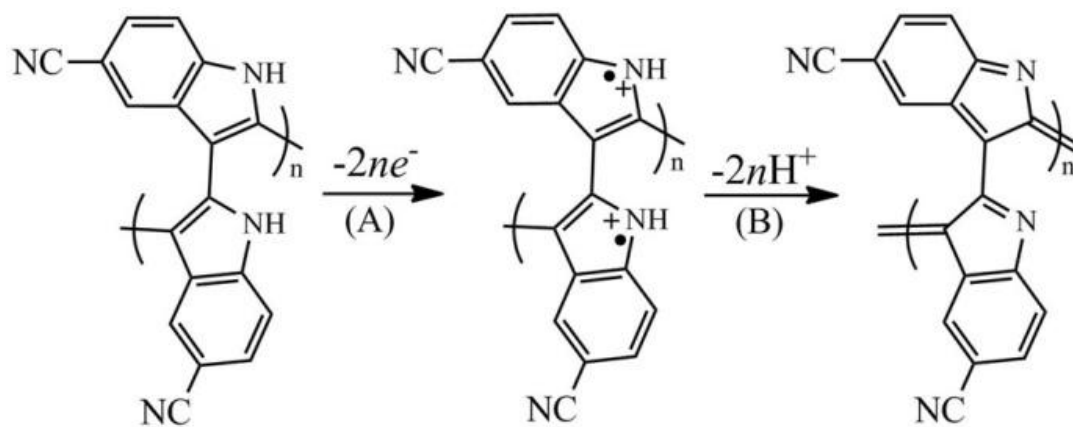


**Figure 5.** Structural evolution of P5CN/GC in H<sub>2</sub>SO<sub>4</sub> solution

Generally, the amount of hydrogen adsorption/desorption on catalyst is directly related to the number of available sites of Pt [13, 41]. In the inset of Fig. 4, the CVs of Pt/GC, Pt-Cu/GC, Pt/P5CN/GC and Pt-Cu/P5CN/GC manifest a pair strong peak (*a*<sub>3</sub>, *c*<sub>3</sub>) between -0.25 and 0.1 V compared with P5CN/GC which are ascribed to the hydrogen adsorption/desorption on the Pt or Pt-Cu nanoclusters surface. The electrochemically surface area (ECSA) of as-prepared catalysts was determined from CV measurements of hydrogen adsorption charge (*Q*<sub>H</sub>) in 0.5 mol L<sup>-1</sup> H<sub>2</sub>SO<sub>4</sub> solution. The ECSA of each catalyst can be estimated by using the equation (2):

$$ECSA = Q_H / \theta_m \quad (2)$$

A charge to metal area conversion factor  $\theta_m$  of 210  $\mu\text{C cm}^{-2}$  for Pt was therefore adopted to compute the ECSA of as-prepared catalysts based on the equation (2) [42, 43]. It can be seen from Table 1, the Pt-Cu/P5CN/GC has the largest *Q*<sub>H</sub> and ECSA, which is believed to be due to the higher dispersion Pt-Cu nanoclusters at the P5CN/GC surface [44]. For the sake of evaluating the specific electrochemically surface area (SECSA), the same Pt loading of 12.5  $\mu\text{g cm}^{-2}$  was used to calculate for as-prepared catalysts. The results in Table 1 show that the SECSA value for Pt-Cu/P5CN/GC is almost three times larger than the bare Pt/GC. Moreover, this value is similar to the result obtained by Chen *et al.* [44], who reported the values 68.7 and 51.1  $\text{m}^2 \text{g}^{-1}$  for Pt/PANi and Pt/C electrode, respectively.

**Table 1.** Comparison of parameters on as-prepared catalysts

1. Catalysts	2. <i>Q</i> <sub>H</sub>	4. ECSA	6. SECSA
	3. / × 10 <sup>-4</sup> C	5. /cm <sup>2</sup>	7. /m <sup>2</sup> g <sup>-1</sup>
8. Pt/GC	9. 1.47	10. 0.89	11. 25.3
12. Pt-Cu/GC	13. 2.12	14. 1.01	15. 28.8
16. Pt /P5CN/GC	17. 3.55	18. 1.69	19. 48.1
20. Pt-Cu/ P5CN /GC	21. 4.52	22. 2.15	23. 61.2

### 3.3. Electrocatalytic activity

It is well known that the catalytic performance of catalyst can be evaluated by the peak current density and potential value of voltammetric curves. For a good electrocatalyst, the higher peak current density and lower peak potential value are favourable for the application in fuel cells. Fig. 6 shows the CVs of as-prepared catalysts for the methanol oxidation reaction (MOR) and formic acid oxidation reaction (FAOR) in 0.5 M H<sub>2</sub>SO<sub>4</sub> with a scan rate of 50 mV s<sup>-1</sup>, respectively. As shown in Fig 6A, the CV profiles present typical characterization of methanol electrooxidation in acid medium. The Table 1 shows the detail information toward the methanol electrooxidation from the Fig. 6A. The onset potential on Pt/P5CN/GC and Pt-Cu/P5CN/GC are about 70 and 110 mV more negative than those without P5CN. The negative shifts meant that the methanol was oxidized easily [12]. The largest hydrogen adsorption/desorption peak was observed with the Pt-Cu/P5CN/GC from -0.25 to 0.05 V, which was in well agreement with the result of Fig 4 and implied that the Pt-Cu/P5CN/GC had more available sites of Pt toward methanol electrooxidation. Simultaneously, the obvious oxidation peaks of methanol can be seen at around 0.62 V, and the peak potentials on the Pt/P5CN/GC and Pt-Cu/P5CN/GC have a slight negative shift which indicates more favourable reaction kinetics on Pt-Cu/P5CN/GC [40, 45]. Moreover, the peak current density on the as-prepared catalysts increased in the order of Pt/GC < Pt-Cu/GC < Pt/P5CN/GC < Pt-Cu/P5CN/GC, suggesting the electron transfer kinetics can be markedly improved by the incorporation of Pt or Pt-Cu nanoclusters on the P5CN surface [46]. It is noticeable that a pair of peaks at 0.9 V is attributed to the proton exchange of P5CN corresponding to the peak (*a*<sub>2</sub>, *c*<sub>2</sub>) in Fig. 4.

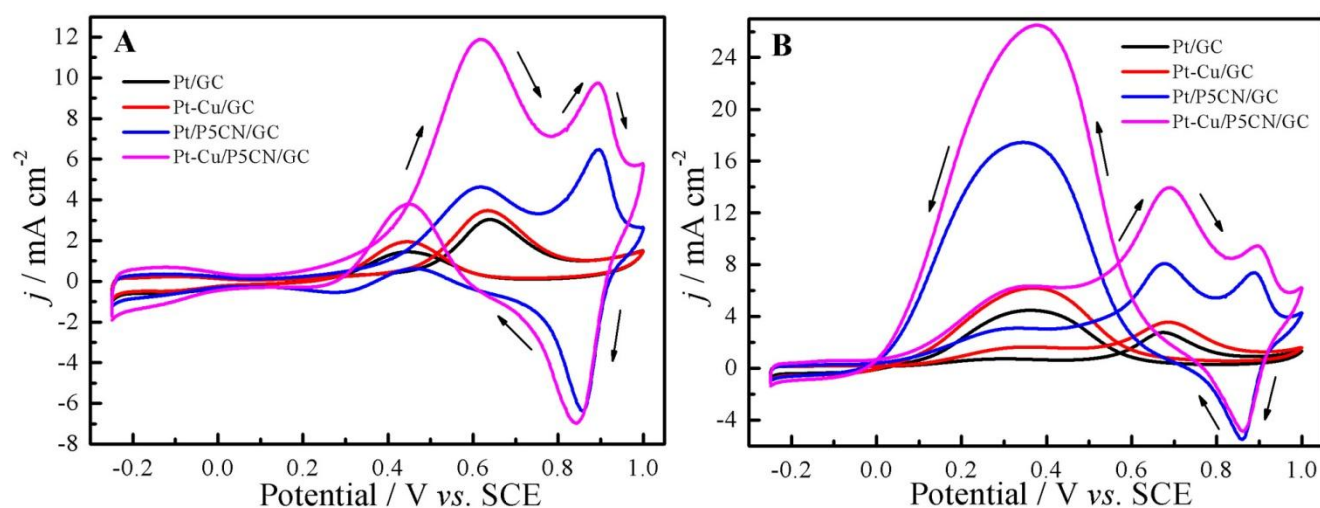
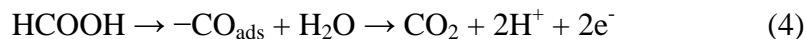
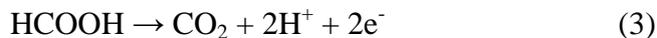


**Figure 6.** CVs on Pt/GC, Pt-Cu/GC, Pt/P5CN/GC and Pt-Cu/P5CN/GC in 0.5 M H<sub>2</sub>SO<sub>4</sub> + 0.5 M CH<sub>3</sub>OH (A) and 0.5 M H<sub>2</sub>SO<sub>4</sub> + 0.5 M HCOOH (B), respectively.

During the formic acid electrooxidation in Fig. 6B, the typical CV profiles on as-prepared catalysts can be clearly observed, which are composed of two forward scan peaks and one backward scan peak. Compared to MOR, the remarkable difference in FAOR depended on the so-called “dual

pathway” reaction mechanism accepted commonly [47, 48]. For the two forward scan peaks, the weak and broad one centred at 0.32 V was attributed to the direct oxidation of formic acid via dehydrogenation pathway (equation 3), while the intensity one at 0.67 V was due to the oxidation of intermediate  $\text{CO}_{\text{ads}}$  formed from the dehydration of formic acid (equation 4) [49].



For the backward scan peak, there presented one broad and intensity peak at 0.36 V which was mainly related to the absence of  $\text{CO}_{\text{ads}}$  poison [5, 36]. Moreover, when the potential scan moved to more negative and came back to the initial forward scan, the surface of Pt particles were anew poisoned by  $\text{CO}_{\text{ads}}$ , resulting in the rapid decrease of peak current density in the dehydrogenation pathway [5]. Meanwhile, the peak current density for both the forward and backward scan increased gradually in the following order: Pt/GC < Pt-Cu/GC < Pt/P5CN/GC < Pt-Cu/P5CN/GC. It also can be found that the values of peak current density on Pt/P5CN/GC and Pt-Cu/P5CN/GC are about 4 times those of the peak current density on Pt/GC and Pt-Cu/GC, and the values on the as-prepared catalysts with Cu are only 1.5 times higher than those without Cu. It is clear that Pt-Cu/P5CN/GC shows the best catalytic performance for FAOR. In addition, the higher catalytic activity for FAOR can be observed than that for MOR in Fig. 6. Recently, many of literatures have demonstrated that the noble metal and alloys as anodic catalysts toward FAOR show better catalytic activities than MOR [5, 50].

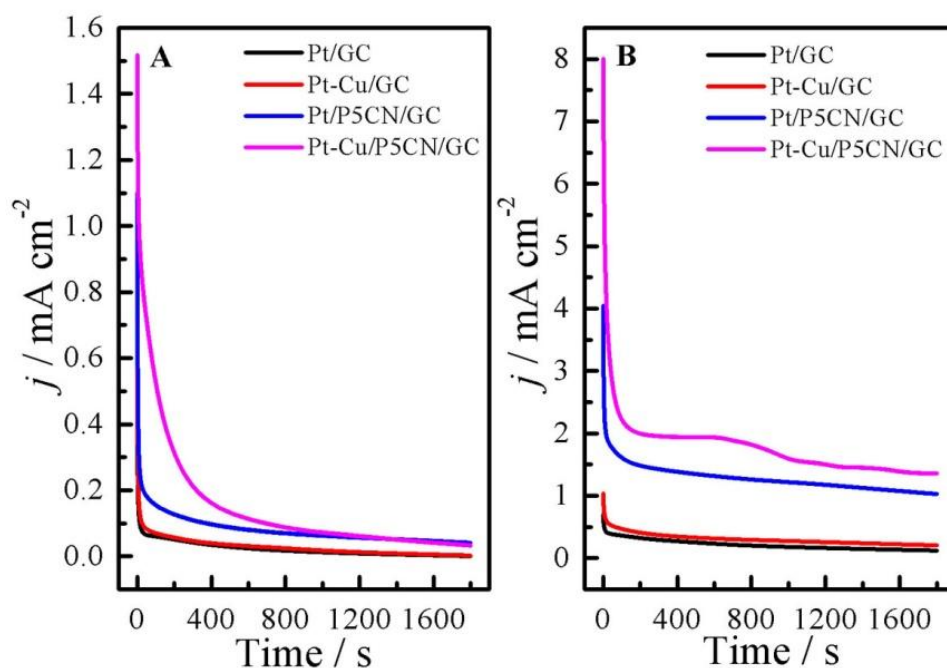


**Figure 7.** Chronoamperometric curves of Pt/GC, Pt-Cu/GC, Pt/P5CN/GC and Pt-Cu/P5CN/GC at 0.4 V in 0.5 M  $\text{H}_2\text{SO}_4$  + 0.5 M  $\text{CH}_3\text{OH}$  (A) and 0.5 M  $\text{H}_2\text{SO}_4$  + 0.5 M  $\text{HCOOH}$  (B), respectively.

To evaluate the stability of as-prepared catalysts for methanol and formic acid oxidation, the chronoamperometry were performed at the potential of 0.4 V. As shown in Fig. 7A and Fig. 7B, the gradual decreasing current density can be seen, and the current density decays rapidly during the initial process of oxidation. The recorded current density is close to the rather steady current profile for about 30 min, which indicates the as-prepared catalyst is stable toward MOR and FAOR [14]. Moreover, one can see that the current density on Pt-Cu/P5CN/GC maintains the largest value among these as-prepared catalysts for both methanol and formic acid oxidation. It is also in well agreement with the result of CVs, indicating the better stability and tolerance to the intermediate species. In addition, the oxidation current density for FAOR is higher than that for MOR on the corresponding catalyst.

Therefore, these results indicated that the introduction of Cu and P5CN had great influence on the electron transfer kinetics on the surface of as-prepared catalysts, and produced a great promotion effect for MOR and FAOR. The fact that the Pt-Cu/P5CN/GC showed the highest electrocatalytic activity toward both MOR and FAOR was attributed to three major factors: (1) the porous P5CN was an excellent electron and proton conducting polymer. It can promoted well the dispersion of Pt-Cu nanoclusters on its surface, and the facile shuttle of electronic charges, and the increase of specific surface area of Pt-Cu nanoclusters, consequently enhanced the utilization of active sites of Pt and catalytic performance; [14, 51, 52] (2) the possible synergistic effect between the Pt-Cu nanoclusters and P5CN; [25, 26] (3) the introduction of Cu into Pt probably changed the electronic ligand-effect and surface crystalline orientation of Pt particles [1, 3, 5].

#### 4. CONCLUSIONS

In present work, Pt-Cu nanoclusters-decorated porous P5CN obtained by a novel electrochemical route has been investigated as an anodic electrocatalyst toward methanol and formic acid oxidation. The porous P5CN was demonstrated to be an excellent electron and proton conducting materials, and promoted well the dispersion of Pt-Cu nanoclusters with the mean diameter of 4.5 nm. It was found that the incorporation of Pt-Cu nanoclusters on the P5CN surface markedly enhanced the electronic transfer and the increase of electrochemical active surface area of Pt-Cu nanoclusters. Thus, the Pt-Cu/P5CN/GC showed the remarkable electrocatalytic activity and stability toward MOR and FAOR. Moreover, the introduction of Cu into the Pt catalysts was also proven to improve slightly the catalytic activity. In addition, we have revealed that the catalytic activity of Pt-Cu/P5CN/GC toward formic acid oxidation was higher than that toward methanol oxidation. Therefore, the Pt-Cu/P5CN/GC is a favourable candidate for the catalytic application.

#### ACKNOWLEDGEMENTS

The authors appreciate the supports of the National Natural Science Foundation of China (Grant Nos. 20933007, 51073114, 51073074 and 50963002), the key scientific project from Ministry of Education, China (2007-207058), the “One Hundred Talents” program of Chinese Academy of Sciences (1029471301), the Opening Project of Xinjiang Key Laboratory of Electronic Information Materials and Devices, the Priority Academic Program Development of Jiangsu Higher Education Institutions,

Natural Science Foundation of Jiangxi province (2007GZH1091), Jiangxi Provincial Department of Education (GJJ08369).

## References

1. S. Papadimitriou, S. Armyanov, E. Valova, A. Hubin, O. Steenhaut, E. Pavlidou, G. Kokkinidis and S. Sotiropoulos, *J. Phys. Chem. C*, 114 (2010) 5217.
2. T. Ghosh, B. M. Leonard, Q. Zhou and F. J. DiSalvo, *Chem. Mater.*, 22 (2010) 2190.
3. D. Xu, S. Bliznakov, Z. Liu, J. Fang and N. Dimitrov, *Angew. Chem. Int. Ed.*, 49 (2010) 1282.
4. C. H. Yen, K. Shimizu, Y.-Y. Lin, F. Bailey, I. F. Cheng and C. M. Wai, *Energy Fuels*, 21 (2007) 2268.
5. H. Yang, L. Dai, D. Xu, J. Fang and S. Zou, *Electrochim. Acta*, 55 (2010) 8000. H. Li, D. Kang, H. Wang and R. Wang, *Int. J. Electrochem. Sci.*, 6 (2011) 1058
6. E. Favry, D. Wang, D. Fantauzzi, J. Anton, D. S. Su, T. Jacobc and N. Alonso-Vante, *Phys. Chem. Chem. Phys.*, 13 (2011) 9201.
7. J. Chen, B. Lim, E. Lee and Y. Xia, *Nano Today*, 4 (2009) 81.
8. E. Antolini and E. R. Gonzalez, *Appl. Catal., A*, 365 (2009) 1.
9. W. Zhou, Y. Du, F. Ren, C. Wang, J. Xu and P. Yang, *Int. J. Hydrogen Energy*, 35 (2010) 3270.
10. F. Ren, W. Zhou, Y. Du, P. Yang, C. Wang and J. Xu, *Int. J. Hydrogen Energy*, 36 (2011) 6414.
11. T. Page, R. Johnson, J. Hormes, S. Noding and B. Rambabu, *J. Electroanal. Chem.*, 485 (2000) 34.
12. W. Zhou, Y. Du, H. Zhang, J. Xu and P. Yang, *Electrochim. Acta*, 55 (2010) 2911.
13. S. Patra and N. Munichandraiah, *Langmuir*, 25 (2009) 1732.
14. R. K. Pandey and V. Lakshminarayanan, *J. Phys. Chem. C*, 113 (2009) 21596.
15. C.-C. Yang, T.-y. Wu, H.-R. Chen, T.-H. Hsieh, K.-S. Ho and C.-W. Kuo, *Int. J. Electrochem. Sci.*, 6 (2011) 1642
16. J.-B. Raoof, M. Jahanshahi and S. M. Ahangar, *Int. J. Electrochem. Sci.*, 5 (2010) 517
17. J.-B. Raoof, R. Ojani and S. R. Hosseini, *Int. J. Hydrogen Energy*, 36 (2011) 52.
18. J. Xu, W. Zhou, J. Hou, S. Pu, L. Yan and J. Wang, *Mater. Chem. Phys.*, 99 (2006) 341.
19. H. Talbi and D. Billaud, *Synth. Met.*, 93 (1998) 105.
20. H. Talbi, D. Billaud, G. Louarn and A. Pron, *Spectrochim. Acta, Part A*, 56 (2000) 717.
21. J.-W. Kim, J.-E. Lee, S.-J. Kim, J.-S. Lee, J.-H. Ryu, J. Kim, S.-H. Han, I.-S. Chang and K.-D. Suh, *Polymer*, 45 (2004) 4741.
22. M. F. Philips, A. I. Gopalan and K.-P. Lee, *Catal. Commun.*, 12 (2011) 1084.
23. W. Zhou, C. Wang, J. Xu, Y. Du and P. Yang, *J. Power Sources*, 196 (2011) 1118.
24. S. Palmero, A. Colina, E. Munoz, A. Heras, V. Ruiz and J. Lopezpalacios, *Electrochem. Commun.*, 11 (2009) 122.
25. H. Yang, T. Lu, K. Xue, S. Sun, G. Lu and S. Chen, *J. Electrochem. Soc.*, 144 (1997) 2302.
26. A. Malinauskas, *Synth. Met.*, 107 (1999) 75.
27. N. Watanabe, J. Morais, S. B. B. Accione, Â. Morrone, J. E. Schmidt and M. C. M. Alves, *J. Phys. Chem. B*, 108 (2004) 4013.
28. T. S. Mkwizu, M. K. Mathe and I. Cukrowski, *Langmuir*, 26 (2010) 570.
29. S. R. Brankovic, J. X. Wang and R. R. Adi, *Surf. Sci.*, 474 (2001) L173.
30. J. Zhang, M. B. Vukmirovic, Y. Xu, M. Mavrikakis and R. R. Adzic, *Angew. Chem. Int. Ed.*, 44 (2005) 2132.
31. J. Zhang, F. H. B. Lima, M. H. Shao, K. Sasaki, J. X. Wang, J. Hanson and R. R. Adzic, *J. Phys. Chem. B*, 109 (2005) 22701.
32. K. Sieradzki, *Science*, 284 (1999) 138.
33. J. Huang, Q. Xie, Y. Tan, Y. Fu, Z. Su, Y. Huang and S. Yao, *Mater. Chem. Phys.*, 118 (2009) 371.

34. L.-M. Huang, W.-H. Liao, H.-C. Ling and T.-C. Wen, *Mater. Chem. Phys.*, 116 (2009) 474.
35. S. Park, Y. Xie and M. J. Weaver, *Langmuir*, 18 (2002) 5792.
36. L. Al-Mashat, K. Shin, K. Kalantar-zadeh, J. D. Plessis, S. H. Han, R. W. Kojima, R. B. Kaner, D. Li, X. Gou, S. J. Ippolito and W. Wlodarski, *J. Phys. Chem. C*, 114 (2010) 16168.
37. K. Zhang, L. L. Zhang, X. S. Zhao and J. Wu, *Chem. Mater.*, 22 (2010) 1392.
38. P. Mani, R. Srivastava and P. Strasser, *J. Phys. Chem. C*, 112 (2008) 2770.
39. C. Xu, R. Wang, M. Chen, Y. Zhang and Y. Ding, *Phys. Chem. Chem. Phys.*, 12 (2010) 239.
40. U. A. Paulus, A. Wokaun, G. G. Scherer, T. J. Schmidt, V. Stamenkovic, N. M. Markovic and P. N. Ross, *Electrochim. Acta*, 47 (2002) 3787.
41. S. Trasatti and O. A. Petrii, *Pure. Appl. Chem.*, 63 (1991) 711.
42. W. Vielstich, H. A. Gasteiger and A. Lamm, *Handbook of Fuel Cells–Fundamentals, Technology and Applications*, John Wiley & Sons, New York (2003).
43. Z. Chen, L. Xu, W. Li, MaheshWaje and Y. Yan, *Nanotechnology*, 17 (2006) 5254.
44. T. D. Jarvi, S. Sriramulu and E. M. Stuve, *Colloids Surf. A*, 134 (1998) 145.
45. J. Cui, D. Sun, W. Zhou, H. Liu, P. Hu, N. Ren, H. Qin, Z. Huang, J. Lin and H. Ma, *Phys. Chem. Chem. Phys.*, 13 (2011) 9232.
46. S. Sun and Y. Yang, *J. Electroanal. Chem.*, 467 (1999) 121.
47. X. Yu and P. G. Pickup, *J. Power Sources*, 182 (2008) 124.
48. A. Capon and R. Parsons, *J. Electroanal. Chem.*, 45 (1973) 205.
49. R. Jayashree, J. Spendelow, J. Yeom, C. Rastogi, M. Shannon and P. Kenis, *Electrochim. Acta*, 50 (2005) 4674.
50. Y. Rhee, *J. Power Sources*, 117 (2003) 35.
51. S. Guo, S. Dong and E. Wang, *Small*, 5 (2009) 1869.